Advanced Composite Materials
Publication details, including instructions for authors and subscription information:
http://www.tandfonline.com/loi/tacm20

Improvement of the burst strength of FW-FRP composite pipes after impact using low-modulus amorphous carbon fiber

Shuichi Wakayama , Satoshi Kobayashi , Noriyuki Kiuchi , Yoshio Sohda & Takayuki Matsumoto

Version of record first published: 02 Apr 2012.

To cite this article: Shuichi Wakayama , Satoshi Kobayashi , Noriyuki Kiuchi , Yoshio Sohda & Takayuki Matsumoto (2002): Improvement of the burst strength of FW-FRP composite pipes after impact using low-modulus amorphous carbon fiber , Advanced Composite Materials, 11:3, 319-330

To link to this article: http://dx.doi.org/10.1163/156855102762506344

Adv. Composite Mater., Vol. 11, No. 3, pp. 319–330 (2003)

Also available online - www.vsppub.com

Improvement of the burst strength of FW-FRP composite pipes after impact using low-modulus amorphous carbon fiber

SHUICHI WAKAYAMA [1], SATOSHI KOBAYASHI [1,*], NORIYUKI KIUCHI [2], YOSHIO SOHDA [2] and TAKAYUKI MATSUMOTO [3]

[1] *Graduate School of Engineering, Tokyo Metropolitan University, 1-1 Minami-Ohsawa, Hachioji-shi, Tokyo 192-0397, Japan*
[2] *Central Technical Research Laboratory, Nippon Mitsubishi Oil Corp., 8 Chidori-cho, Naka-ku, Yokohama 231-0815, Japan*
[3] *Nippon Graphite Fiber Corp., Nisseki Mitsubishi Bldg., 1-3-12 Nishi-Shimbashi, Minato-ku, Tokyo 105-8412, Japan*

Received 27 June 2002; accepted 21 October 2002

Abstract—Impact tests of filament-wound carbon fiber reinforced plastic (FW-CFRP) composite pipes were carried out using a drop-weight impact test device developed by the authors. Burst pressure of composite pipes after impact tests was also measured in order to investigate the burst strength degradation due to impact damage. Depth of fiber breakage region caused by impact loading was evaluated after burst strength test. The burst strength of FW-CFRP composite pipes after impact was demonstrated to decrease with the increase in cross-sectional area of damage. Furthermore, low-modulus carbon fibers were wound on the surface of the pipes in order to suppress the impact damage. Consequently, it was understood that the residual burst strength was enhanced due to the reduction of impact damage such as fiber breakages.

Keywords: FW-FRP composite pipe; impact test; burst strength; low-modulus amorphous carbon fiber.

1. INTRODUCTION

Fiber reinforced plastics (FRP) pressure vessels fabricated by filament winding (FW) technology are extensively used because of their practical advantages, such as light weight and high strength compared with seamless steel vessels. In the case of daily use of FW-FRP vessels, there are possibilities of impact loading such as dropping and/or knocking vessels. To avoid damage in such circumstances, it is necessary to clarify the strength reduction mechanism after impact and to improve

*To whom correspondence should be addressed. E-mail: wakayama@ecomp.metro-u.ac.jp

the impact resistance. There have been some investigations for burst strength reduction after impact [1–4]. Most studies dealt with surface fiber breakage length, although fiber break depth is also influential on the burst strength.

Therefore, improvement of the impact tolerance is still necessary for the FW-FRP vessels. Previous investigations, including that of the present authors [5], indicated that dominant damage due to impact was fiber micro-buckling caused by compressive stress. When the impact load is applied to the pressure vessel, the convex vessel wall is deformed into a concave shape and the surface layer of the vessel is subjected to large compressive strain compared with composite plate structures. Therefore, it is expected that the application of fibers with high compressive strength into the surface layers would enhance the impact tolerance and the residual strength after impact of FW-FRP pressure vessels.

In the present study, internal pressure tests on FW-CFRP composite pipes after impact test were conducted. In order to improve the impact tolerance, low modulus amorphous carbon fibers, which have high compressive strain to failure, were applied to the surface of composites pipes. Impact damage, which consists of fiber break length and depth, was evaluated as a function of absorbed energy. Consequently, the effectiveness of the hybridization on the impact tolerance was investigated.

2. EXPERIMENTAL PROCEDURES

Composite pipes were fabricated using a filament winding machine and used for the specimens illustrated in Fig. 1. Specimens consisted of aluminum alloy (A6063-T6) liner and CFRP layer. Carbon fiber used was Torayca T700S-24K supplied by Toray Inc. and epoxy resin Epikote 828 supplied by Japan Epoxy Resin Co. was used for matrix. In order to improve the impact resistance, low modulus amorphous carbon fiber Granoc XN05-30S, supplied by Nihon Graphite fiber Inc., was wound on the surface of the composite pipes. Table 1 indicates mechanical properties of the fiber

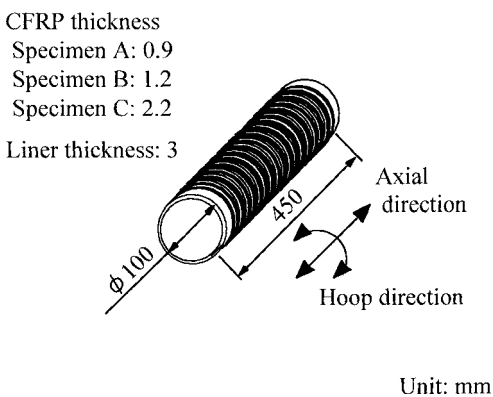

Figure 1. Schematic drawing of composite pipe.

and compressive properties of the unidirectional composites. XN05 composite has high compressive strain and it was reported that hybrid composite using XN05 has high impact resistance properties [6].

Three types of specimens were prepared. Table 2 shows specimen configurations. Specimen A consisted of five T700S-24K layers and aluminum liner and Specimen B had two additional XN05-30S layers on the surface. Specimen C was designed to be equivalent strength of Specimen A and it had four T700S layers and nine XN05 layers.

Figure 2 shows the drop-weight impact tests apparatus. Mass and initial height of the impactor were 7 kg and 0.45 m, respectively, i.e. the potential energy of the impactor was 30 J. Impactor radius, R, was selected as 3, 10 and 20 mm for Specimen A, and 3 and 10 mm for Specimens B and C. Absorbed energy was calculated from the difference between initial height and maximum rebound height of impactor measured by video camera. Some of the specimens after impact tests were sectioned and observed by optical microscopy.

The residual strength of composite pipes was measured by internal pressure tests using the test apparatus illustrated in Fig. 3. In the present study, strength of hoop direction is of most concern and axial strength is very weak; therefore the deformation in the axial direction was constrained by the stiff shaft centered in the pipes. Figure 4 shows the internal pressure tests system. The specimen was set in the test apparatus and placed in the container. Strain gauges were glued on the

Table 1.
Material properties

Fiber designation		Granoc XN-05	T700S
Fiber properties	Tensile strength (MPa)	1180	4900
	Tensile modulus (GPa)	55	230
	Strain to failure (%)	2.0	2.1
	Density (Mg/m^3)	1.65	1.8
	CTE (10^{-6}/K)	3.4	−0.4
Composites properties (Matrix: 130°C epoxy)	Tensile strength (MPa)	640	2650
	Tensile modulus (GPa)	34	127
	Tensile strain to failure (%)	1.83	1.7
	Compressive strength (MPa)	870	1400
	Compressive modulus (GPa)	32	129
	Compressive strain to failure (%)	2.9	1.4

Table 2.
Specimen configuration

Specimen A	A6063-T6 + T700S-24K $[0^\circ_5]$
Specimen B	A6063-T6 + T700S-24K $[0^\circ_5]$ + XN-05-30S $[0^\circ_2]$
Specimen C	A6063-T6 + T700S-24K $[0^\circ_4]$ + XN-05-30S $[0^\circ_9]$

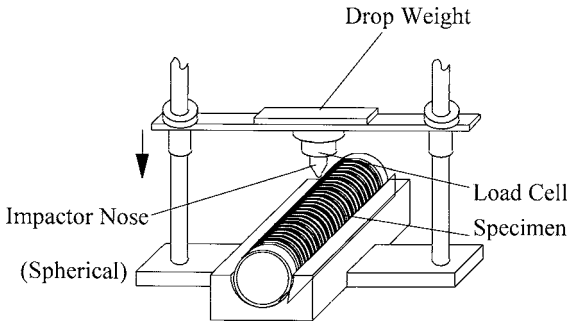

Figure 2. Impact tests apparatus.

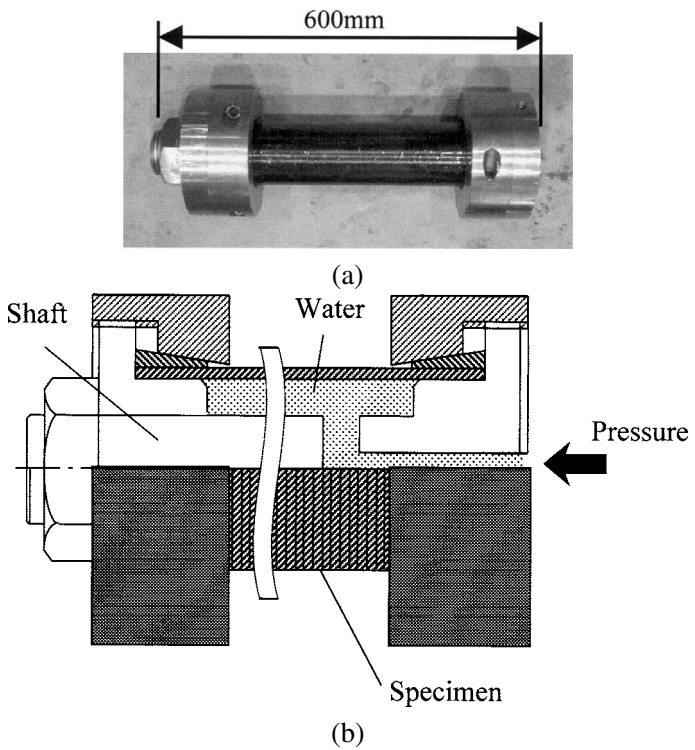

Figure 3. Internal pressure tests apparatus ((a) photograph of the specimen with pressure test apparatus, (b) schematic drawing of pressure test apparatus).

specimen at 10, 30 and 50 mm apart from the impact point and on the opposite side. The surface of the specimen was observed by video camera during the internal pressure test. Acoustic emission was also measured to detect microscopic damage. The number of specimens for each test condition was five or six.

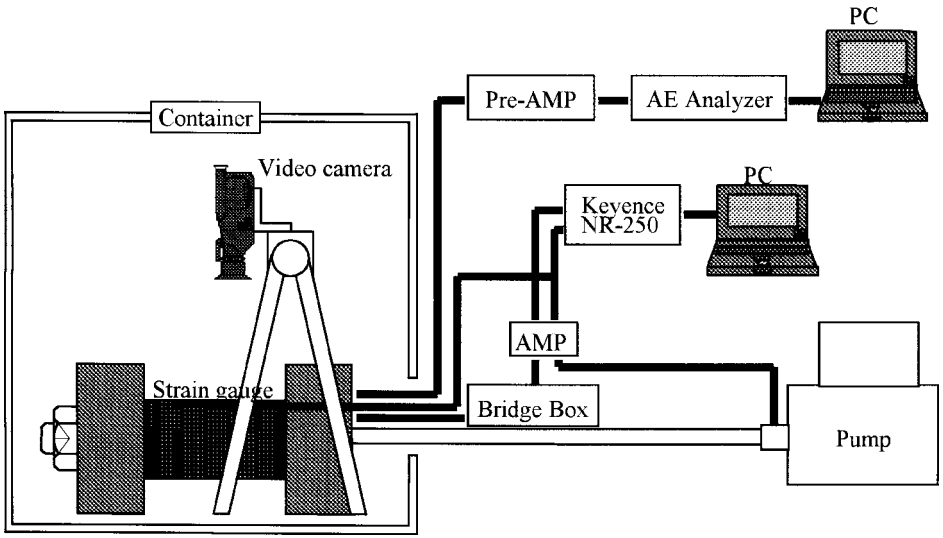

Figure 4. Internal pressure test system.

3. EXPERIMENTAL RESULTS AND DISCUSSION

3.1. Impact tests

Figure 5 shows the schematic drawings of surface damage after impact tests. Splitting and/or fiber breakages were observed around indentations except for the case of $R = 20$ mm for Specimen A, where no damages were observed. Fiber breakage were observed only in the Specimen A with $R = 10$ mm. Damage areas in Specimens A and B were larger in the case of $R = 10$ mm, while there was no difference in damage area in Specimen C. It is significant that the damage area in Specimen C was smaller than in Specimens A and B, which suggests the effectiveness of the XN-05 layer against impact loading.

The average absorbed energy during impact tests are shown in Fig. 6. As can be seen in the figure, absorbed energy decreased with increasing impactor radius. However, the absorbed energy in Specimens A and B with same impactor radius are equivalent, although the impact damage in Specimen A is larger, as shown in Fig. 5. It is then understood that most of the impact energies were dissipated by the plastic deformation of aluminum liners, which is consistent with the previous result [5]. On the other hand, the absorbed energy of Specimen C was smaller than for Specimens A and B. This might be attributed to the larger bending rigidity of Specimen C, which results in smaller deformation of aluminum liner.

To investigate the feature of impact damage, the fiber damage length was estimated from the surface observation (Fig. 5). If the fiber breakage was not observed, the diameter of indentation was taken as the damage length. Figure 7 shows fiber damage length as a function of absorbed energy. It can be understood from the figure that the damage length of the specimen with thicker XN-05 layer is smaller within close absorbed energy values.

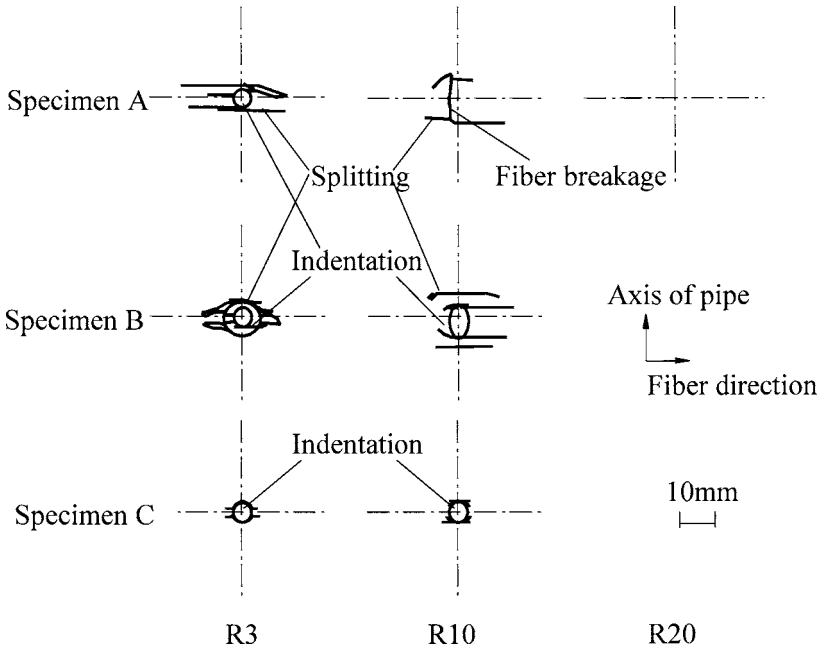

Figure 5. Schematic drawings of surface damages caused by impact tests.

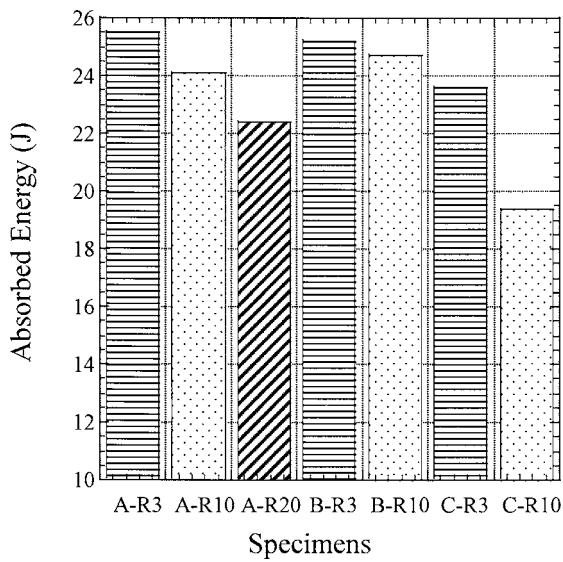

Figure 6. Absorbed energy in the impact tests. Specimen names and the radius of impactor are indicated, e.g. A-R3 is the Specimen A after impact loading with the impactor of 3 mm diameter.

In order to obtain information on the damage in more detail, the cross-section of Specimen A after the impact test for the impactor diameter of 3 mm (absorbed energy was 25.9 J) was observed as shown in Fig. 8. It is observed in Fig. 8a

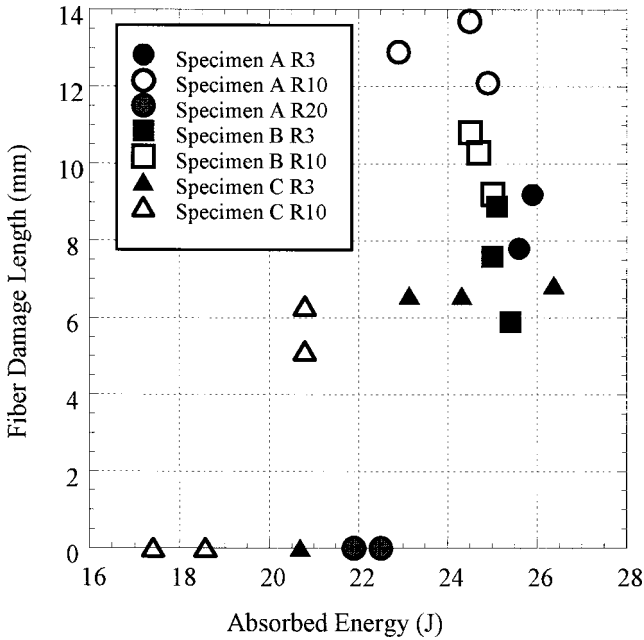

Figure 7. Fiber damage length as a function of absorbed energy.

that the aluminum liner was deformed plastically and the delamination between CFRP layer and metal liner occurred by the elastic recovery of CFRP after impact loading. In the enlarged photograph (Fig. 8b), fiber breakages due to micro-buckling and interlaminar delamination were observed below the indentation regions. It is important that those fiber breakages could not be observed in Specimens B and C. Although further investigations on the nucleation mechanisms of impact damages are needed, it was deduced that the impact damage was suppressed by XN-05 layers.

3.2. Internal pressure tests

A typical result of the internal pressure test after impact is shown in Fig. 9, where the Specimen A with the impact load by the impactor with radius of 10 mm was used and the absorbed impact energy was 24.5 J. Figures 9a and b show the strain and AE cumulative events, respectively and (c-1) to (c-3) show the fracture behavior observed on the surface.

In the strain behavior at 10 mm from the impact point (Fig. 9a), the compressive deformation in initial loading stage was observed. This is considered to be the result of unbending deformation of the dented part of the aluminum liner.

During the internal pressure test, the strain discontinuities were observed as indicated in Fig. 9a at 32 MPa (c-1) and 37 MPa (c-2). It can be seen in Fig. 9b that AE cumulative events increased rapidly at corresponding pressure. While no fracture behavior was observed on the surface (c-1) at 32 MPa, strain and AE behavior suggest that the internal damage were initiated and/or grew. On the other

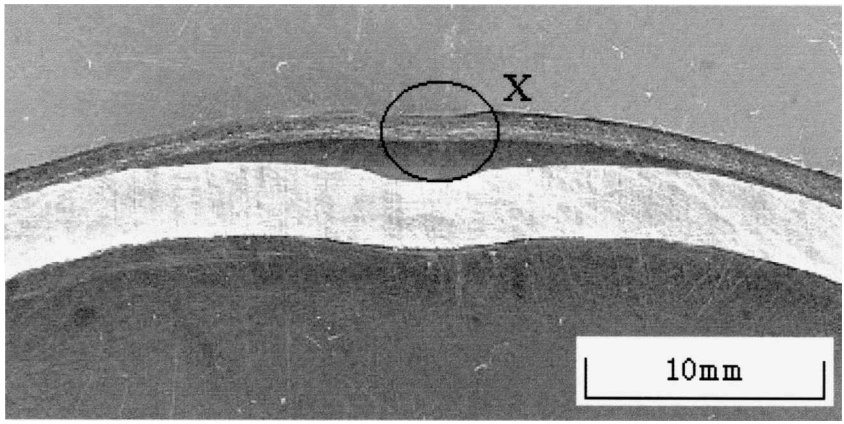

(a) Overview

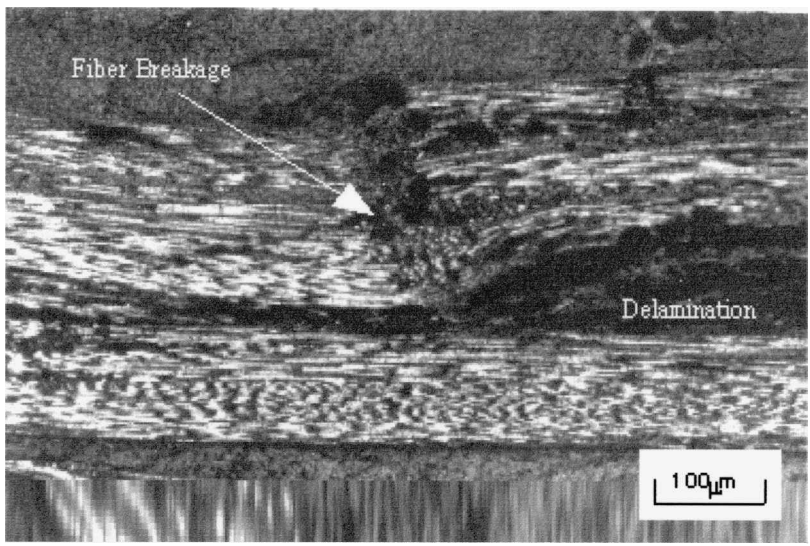

(b) Enlargement of X

Figure 8. Result of cross-sectional damage observation. (Specimen A, R: 3 mm, Absorbed energy: 25.9 J)

hand, the initiation of splitting was observed at 37 MPa (c-2) corresponding to strain and AE behavior. Finally, the additional initiation of splitting and the corresponding rapid increase in AE were observed at 40 MPa (c-3) and it grew to final failure.

This fracture behavior was observed on the surface only for Specimen A with the impact damage by the impactor of $R = 3$ or 10 mm. In other specimens, little damage progress was observed on the surface, although AE activities such as rapid increasing points were detected prior to final burst in all specimens, which suggest the progress of internal damage, such as delamination. It is then noted that

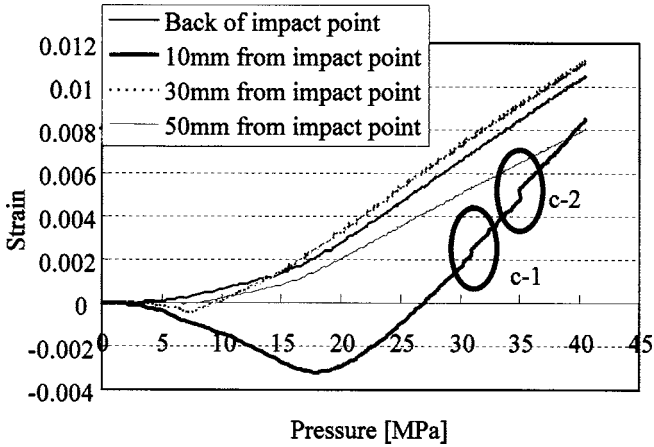

(a) Strain as a function of pressure

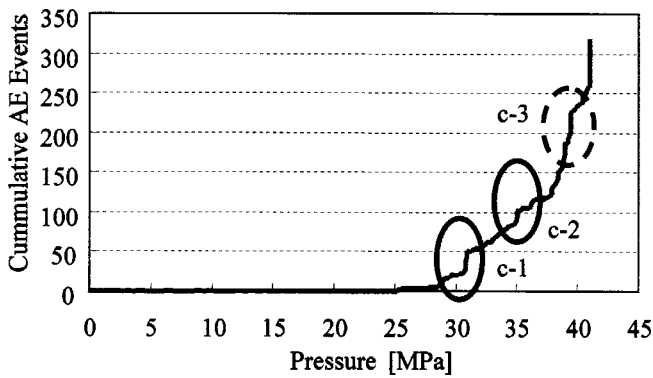

(b) Cummulative AE events as a function of pressure

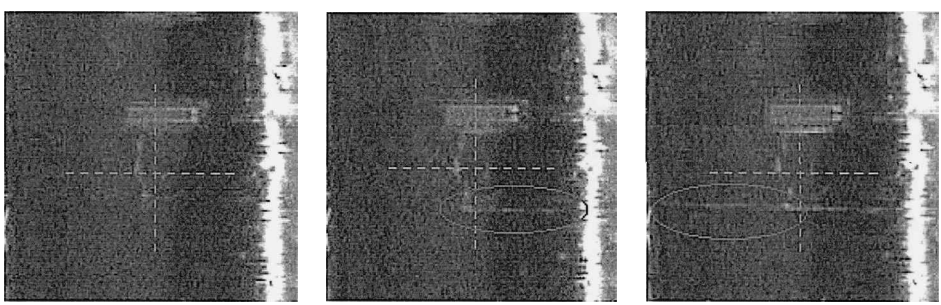

(c-1) 32 MPa (c-2) 37 MPa (c-3) 40 MPa

Figure 9. Result of internal pressure tests. (Specimen A, R: 3 mm, Absorbed energy: 24.5 J.)

AE measurement is the most sensitive way to detect the fracture behavior during internal burst test of pressure vessels.

The average burst strength of the specimens before and after impact tests is shown in Fig. 10. It can be seen in the figure that the virgin burst strengths of Specimens

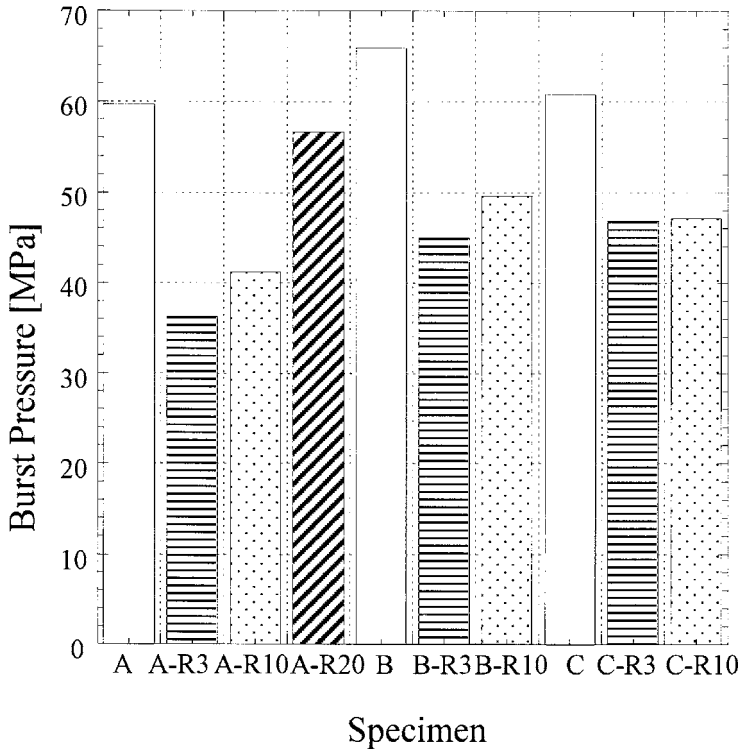

Figure 10. Residual burst strength of composite pipes after impact tests. The burst strength of specimens without impact loading (A, B and C) are also shown.

A and C are almost equal but then Specimen C was well designed and fabricated. It is also understood that the larger the impactor radius, the higher is the residual strength.

In order to clarify the effect of low modulus amorphous fiber on the impact resistance, the residual strength ratio, which is defined as strength after impact normalized by strength of virgin specimen, is calculated and shown in Fig. 11. Residual strength ratios of Specimens B and C were larger than for Specimen A. Furthermore, the difference in residual burst strength ratio of Specimen C was smaller than others. Consequently, it can be concluded that the impact resistance of FW-FRP composite pipes was enhanced by XN-05 fibers.

On the fracture surface of Specimen A, fiber damage region caused by impact loading could be distinguished from the fracture surface during internal pressure. The damage area was then measured as the product of fiber breakage depth and fiber breakage length observed on the surface. Figure 12 shows the relation between strength ratio and cross-sectional area of fiber breakage. As can be seen in the figure, strength ratio linearly decreased as damage area increased. Unfortunately, the damage depth of Specimens B and C was too small to measure, so further investigations are required for the precise evaluation of damage depth in Specimen B

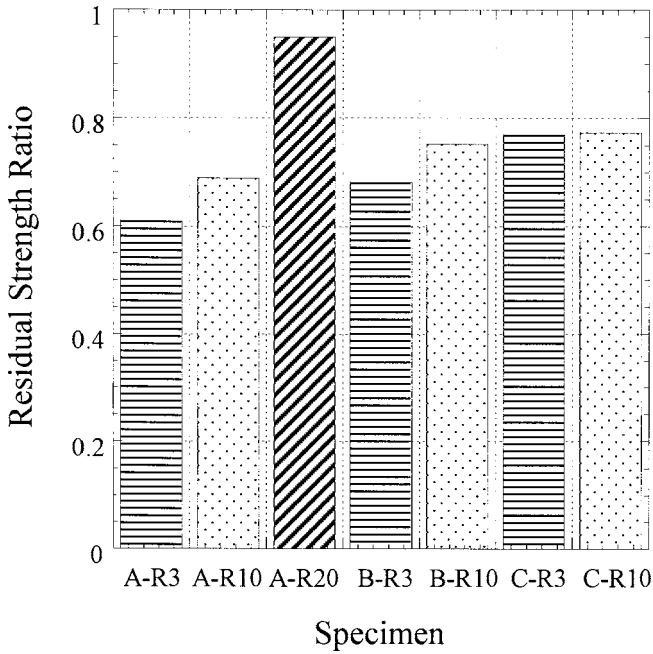

Figure 11. Residual strength ratio.

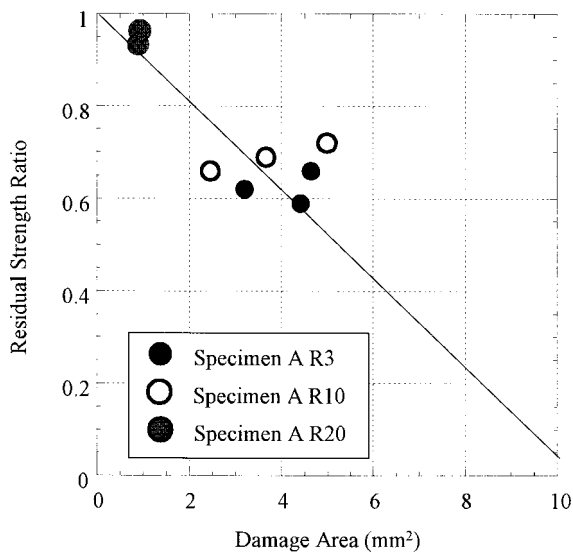

Figure 12. Residual strength ratio as a function of damage area.

and C. However, it was understood that the depth profile of impact damage as well as length is significant for the characterization of strength degradation of pressure vessel with impact damage.

4. CONCLUSION

In the present study, drop-weight impact tests and subsequent internal pressure tests of FW-CFRP composite pipes were carried out. Especially, the effect of low-modulus amorphous carbon (XN-05) fiber on impact damage tolerance was investigated. Finally, the following conclusions were obtained.

(1) Impact damage observed on the surface was decreased by XN-05 fibers. Especially, fiber breakage under the impact point was not observed in the specimens with XN-05 layers.

(2) Impact absorbed energy become larger as the radius of the impactor become smaller. However, XN-05 layers had little effect on the absorbed energy, since the work for plastic deformation was dominant within the energy in this study.

(3) The degradation of residual burst strength could be suppressed by applying low modulus amorphous carbon fiber on the surface of the pipes.

Acknowledgement

The authors would like to acknowledge the support form the Grant in Aid for Scientific Research (No. 12555181), Japan Society for the Promotion of Science.

REFERENCES

1. A. P. Christoforou and S. R. Swanson, Strength loss in composite cylinder under impact, *Trans. ASME* **110**, 180 (1988).
2. K. L. Alderson and K. E. Evans, Low velocity transverse impact of filament-wound pipes: Part 1. Damage due to static and impact loads, *Composite Structures* **20**, 37 (1992).
3. S. A. Matemilola and W. J. Stronge, Low-speed impact damage in filament-wound CFRP composite pressure vessels, *J. Pressure Vessel Technology* **119**, 435 (1997).
4. J. Curtis, M. J. Hinton, S. Li, S. R. Reid and P. D. Soden, Damage, deformation and residual burst strength of filament wound composite tubes subjected to impact or quasi-static indentation, *Composites Part B* **31**, 419 (2000).
5. T. Takekusa, S. Kobayashi, N. Akkus, S. Wakayama and T. Takehana, Experimental characterization of burst strength of FW-FRP composite vessel after impact, in: *Proc. 25th Symp. Compos. Mater.*, Japan–Korea Joint Session, p. 113 (2000).
6. N. Kiuchi, Y. Sohda, T. Matsumoto, G. Ishikawa and Y. Arai, The improvement of impact properties of hybrid CFRP with amorphous carbon fiber, in: *Proc. 25th Symp. Compos. Mater.*, Japan–Korea Joint Session, p. 91 (2000).